CRYSTAL GROWTH & DESIGN
2009
VOL. 9, NO. 7
3327–3332

Structural Variation in Porphyrin Pillared Homologous Series: Influence of Distinct Coordination Centers for Pillars on Framework Topology

Haemi Chung,[†] Paul M. Barron,[†] Richard W. Novotny,[†] Hyun-Tak Son,[†] Chunhua Hu,[‡] and Wonyoung Choe*,[†]

Department of Chemistry, University of Nebraska—Lincoln, Lincoln, Nebraska 68588-0304, and Department of Chemistry, New York University, New York, New York 10003-6688

Received February 20, 2009; Revised Manuscript Received April 11, 2009

ABSTRACT: A new series of porphyrin paddlewheel frameworks (PPFs) has been assembled from 5,10,15,20-tetrakis(4-carboxyl)-21*H*,23*H*-porphine (TCPP), $Zn(NO_3)_2 \cdot 6H_2O$, and organic pillars such as *N*,*N*′-di-(4-pyridyl)-1,4,5,8-naphthalenetetracarboxydiimide (DPNI) and 3,6-di-4-pyridyl-1,2,4,5-tetrazine (DPT). Here we report the synthesis and structural characterization of five new PPFs based on 2D porphyrin paddlewheel grid. In this homologous series, the stacking patterns of such 2D porphyrin sheets are varied and exhibit two new structures, namely, bilayer and interpenetrated AA stacking pattern, in addition to the ABBA pattern previously observed.

Introduction

The field of metal−organic frameworks (MOFs) has experienced explosive growth in the past decade, mainly due to their fascinating framework topologies and potentially interesting physical properties in applications, such as hydrogen storage, catalysis, and magnetism.[1−4] To build such MOFs, the choice of secondary building units (SBUs) is extremely important. In many cases, these SBUs play a key role in directing the final framework topology and make a significant impact on mechanical and physical properties of the resulting MOFs.[5,6] For example, tetranuclear $Zn_4O(COO)_6$ SBU generally accepts carboxylate-based linkers and often forms mechanically rigid, α-Po type frameworks.[5] In contrast, dinuclear $M_2(COO)_4$ paddlewheel SBUs (M = Co, Ni, Cu, Zn, Cd, Mn) offer two distinct coordination centers for organic linkers: one for carboxylate- and the other for pyridyl-based organic building blocks.[7−10] Assembly of these two types of organic linkers, together with paddlewheel SBUs, results in a series of 3D pillared paddlewheel frameworks.[7−10] Creating additional binding sites for organic linkers offers a powerful tunable feature in MOF structures that may be highly desirable for rational design of functional MOF materials.

We are particularly interested in a new synthetic strategy to construct MOFs with multiple ligand coordination centers.[11−13] To this end, porphyrins are excellent ligands. These macrocycles can accommodate metal centers into the porphyrin cores and can provide additional coordination sites for the organic linkers.[14] Previously, we developed a series of 3D porphyrin paddlewheel frameworks (PPFs), assembled from 5,10,15,20-tetrakis(4-carboxyl)-21*H*,23*H*-porphine (TCPP), $M_2(COO)_4$ paddlewheel SBUs (M = Zn, Co), and 4,4′-bipyridine (BPY) pillar.[13] In this series, the metal center in the porphyrin linker (TCPP) governs the structure formation and systematically controls the stacking pattern of porphyrin paddlewheel sheets, which is unprecedented in other known 3D pillared paddlewheel frameworks.

As a continuing effort to build highly tailored porphyrin-based frameworks, we report a systematic investigation of new porphyrin-based MOFs with two longer pillars, *N*,*N*′-di-(4-pyridyl)-1,4,5,8-naphthalenetetracarboxydiimide (DPNI) and 3,6-di-4-pyridyl-1,2,4,5-tetrazine (DPT). Solvothermal reactions in a solvent mixture, *N*,*N*-diethylformamide (DEF)/ethanol or *N*,*N*-dimethylformamide (DMF)/ethanol yield five new PPFs (Scheme 1). To our surprise, two new structural topologies, bilayer and interpenetrated AA stacking pattern, are found. Their structural relationships are presented here.

Scheme 1. Organic Building Blocks for Pillared Porphyrin Paddlewheel Frameworks

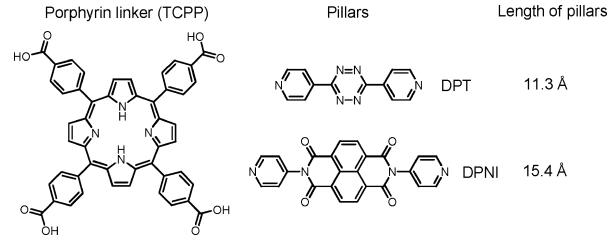

Experimental Section

General Methods. All reactants and solvents are commercially available and used without further purification. ^{1}H NMR spectra were obtained on a 400 MHz Bruker Avance spectrometer using the residual trifluoroacetic acid (11.5 ppm) as an internal reference. Signals are reported as d (doublet) and s (singlet). Coupling constants (*J*) are reported in hertz (Hz). X-ray powder diffraction data were collected on a Rigaku D/Max-B diffractometer with Cu Kα radiation ($\lambda = 1.544$ Å). Single crystal X-ray data for all new crystals were collected. Each crystal was sealed in a capillary for the measurement. Geometry and intensity data were obtained at room temperature with a Bruker SMART Apex CCD area detector diffractometer. Preliminary lattice parameters and orientation matrices were obtained from three sets of frames. Data were collected using graphite-monochromated and MonoCap-collimated Mo Kα radiation ($\lambda = 0.71073$ Å) with the ω scan method.[15] Data were processed with the SAINT+ program[16] for reduction and cell refinement. Multiscan absorption corrections were applied to the data set by using the SADABS program for area detector.[17] The structure was solved by direct method and refined using SHELXTL.[18] Disordered, independent solvent molecules inside the frameworks were eliminated in the refinement by PLATON/SQUEEZE.[19] All atoms were refined with anisotropic displacement parameters. Further details of the refinement data are listed in Table 1.

* Corresponding author. E-mail: choe2@unl.edu.
[†] University of Nebraska—Lincoln.
[‡] New York University.

10.1021/cg900220g CCC: $40.75
Published on Web 05/05/2009

Table 1. Single Crystal Data for Porphyrin Paddlewheel Frameworks

complex	PPF-18	PPF-19	PPF-20	PPF-21	PPF-22
formula[a]	$C_{72}H_{38}N_8O_{13}Zn_3$	$C_{72}H_{38}N_8O_{13}Zn_3$	$C_{84}H_{42}N_{10}O_{14}Zn_3$	$C_{60}H_{34}N_{10}O_9Zn_3$	$C_{66}H_{36}N_{13}O_8Zn_3$
formula weight[a]	1419.27	1419.27	1611.39	1235.08	1335.19
crystal system	tetragonal	monoclinic	tetragonal	tetragonal	tetragonal
space group	*P4/nmm*	*C2/m*	*I4/mmm*	*P4/nmm*	*I4/nmm*
a (Å)	16.7134(2)	22.2897(9)	16.7065(6)	16.598(3)	16.6790(4)
b (Å)	16.7134(2)	16.8927(7)	16.7065(6)	16.598(3)	16.6790(4)
c (Å)	30.8966(6)	16.4976(7)	87.680(6)	26.869(9)	71.0521(18)
α (deg)	90	90	90	90	90
β (deg)	90	104.079(2)	90	90	90
γ (deg)	90	90	90	90	90
V (Å^3)	8630.6(2)	6025.3(4)	24472(2)	7402(3)	19765.9(8)
Z	2	2	4	2	4
ρ_{calc} (g/cm^3)[a]	0.546	0.782	0.437	0.554	0.449
μ (mm^{-1})[a]	0.441	0.631	0.314	0.507	0.382
R1, $I > 2\sigma(I)$	0.0472	0.0466	0.0644	0.0562	0.0704
wR2, $I > 2\sigma(I)$	0.1384	0.1543	0.1909	0.1501	0.2369

[a] Based on the formula without uncoordinated guest solvent molecules.

***N,N′*-Di-(4-pyridyl)-1,4,5,8-naphthalenetetracarboxydiimide (DPNI).**[20] 1,4,5,8-Naphthalenetetracarboxylic dianhydride (0.805 g, 3.00 mmol) and 4-aminopyridine (0.847 g, 6.00 mmol) were dissolved in *N,N*-dimethylacetamide (DMA, 150 mL) in a 250 mL round-bottom flask. The solution was stirred overnight at 135 °C under Ar atmosphere. After the reaction mixture cooled to room temperature, the solution was poured onto diethyl ether (600 mL). The precipitate was filtered and washed with diethyl ether. The product was dried under vacuum to yield 0.900 g (71% yield). ^{1}H NMR (400 MHz, CF_3COOD): δ 8.996 (d, J = 3 Hz, 4H), 8.909 (s, 4H), 8.243 (d, J = 3 Hz, 4H).

PPF-18. 5,10,15,20-Tetrakis(4-carboxyl)-21*H*,23*H*-porphine (7.9 mg, 0.01 mmol), zinc nitrate hexahydrate (8.9 mg, 0.03 mmol), *N,N′*-di-(4-pyridyl)-1,4,5,8-naphthalenetetracarboxydiimide (4.2 mg, 0.01 mmol), and 1.0 M nitric acid (50 μL, 0.05 mmol) in ethanol were dissolved in a mixture of DEF and ethanol (2.0 mL, v/v 3:1). The mixture was sealed in a small capped vial and sonicated to ensure homogeneity. The vial was heated at 80 °C in an oven for 24 h, followed by slow-cooling to room temperature for 9 h.[21]

PPF-19. 5,10,15,20-Tetrakis(4-carboxyl)-21*H*,23*H*-porphine (7.9 mg, 0.01 mmol), zinc nitrate hexahydrate (8.9 mg, 0.03 mmol), *N,N′*-di-(4-pyridyl)-1,4,5,8-naphthalenetetracarboxydiimide (8.4 mg, 0.02 mmol), and 1.0 M nitric acid (30 μL, 0.03 mmol) in ethanol were dissolved in a mixture of DMF and ethanol (2.0 mL, v/v 2:3). The mixture was sealed in a small capped vial and sonicated to ensure homogeneity. The vial was heated at 80 °C in an oven for 24 h, followed by slow-cooling to room temperature for 9 h.[21]

PPF-20. 5,10,15,20-Tetrakis(4-carboxyl)-21*H*,23*H*-porphine (7.9 mg, 0.01 mmol), zinc nitrate hexahydrate (8.9 mg, 0.03 mmol), *N,N′*-di-(4-pyridyl)-1,4,5,8-naphthalenetetracarboxydiimide (16.8 mg, 0.04 mmol), and 1.0 M nitric acid (30 μL, 0.03 mmol) in ethanol were dissolved in a mixture of DMF and ethanol (2.0 mL, v/v 3:1). The mixture was sealed in a small capped vial and sonicated to ensure homogeneity. The vial was heated at 80 °C in an oven for 24 h, followed by slow-cooling to room temperature for 9 h.[21]

PPF-21. 5,10,15,20-Tetrakis(4-carboxyl)-21*H*,23*H*-porphine (7.9 mg, 0.01 mmol), zinc nitrate hexahydrate (8.9 mg, 0.03 mmol), 3,6-di-4-pyridyl-1,2,4,5-tetrazine (4.7 mg, 0.02 mmol), and 1.0 M nitric acid (30 μL, 0.03 mmol) in ethanol were dissolved in a mixture of DEF and ethanol (2.0 mL, v/v 2:1). The mixture was sealed in a small capped vial and sonicated to ensure homogeneity. The vial was heated at 80 °C in an oven for 24 h, followed by slow-cooling to room temperature for 9 h.[21]

PPF-22. 5,10,15,20-Tetrakis(4-carboxyl)-21*H*,23*H*-porphine (8.0 mg, 0.01 mmol), zinc nitrate hexahydrate (9.3 mg, 0.03 mmol), 3,6-di-4-pyridyl-1,2,4,5-tetrazine (11.5 mg, 0.05 mmol), 1.0 M nitric acid in ethanol (60.0 μL, 0.06 mmol) were dissolved in a mixture of DMF and ethanol (2.0 mL, v/v 2:1). The mixture was sealed in a small capped vial and sonicated to ensure homogeneity. The vial was heated at 80 °C in an oven for 24 h, followed by slow-cooling to room temperature for 9 h.[21]

Results and Discussion

Solvothermal reactions of TCPP, $Zn(NO_3)_2 \cdot 6H_2O$, and HNO_3 with DPNI pillar yielded three PPFs (PPF-18, PPF-19, and PPF-20), and similar reactions with DPT yielded two PPFs (PPF-21 and PPF-22). All PPF crystals were obtained after heating at 80 °C for 24 h, followed by slow-cooling to room temperature for 9 h. The amount of reagents and solvents in solvothermal condition has beefn systematically varied to find an optimal synthetic condition for each phase.

The initial molar ratio of the reactants (TCPP/Zn/DPNI) was set to 1:3:1 in DMF/ethanol. A close visual inspection of the product revealed that the product contained two phases with different morphology, platelet (PPF-18) and needle (PPF-19). To optimize the formation of PPF-18, the synthetic conditions were varied. Adding more acid promoted PPF-18 formation, as did the use of DEF instead of DMF. The best synthetic condition for PPF-18 was TCPP/Zn/DPNI/HNO_3 with a molar ratio of 1:3:1:5 in DEF/ethanol solvent mixture. Under this condition, the product appeared to be a single phase from the X-ray powder pattern (see Figure S1 in the Supporting Information). However, visual inspection under an optical microscope indicated that the sample was slightly contaminated by a few needle crystals of PPF-19. To obtain a single phase of PPF-19, the ratio of the cosolvent (DMF/ethanol) was changed. A higher concentration of ethanol favored the formation of PPF-19 as a major phase. The best synthetic condition for PPF-19 was TCPP/Zn/DPNI/HNO_3 with a ratio of 1:3:2:3 in DMF/ethanol (see Figure S2 in the Supporting Information for the X-ray powder pattern). Interestingly, when the concentration of DPNI increases, a new reflection (2θ = 4.15°) appears in the X-ray powder pattern, together with the PPF-18 and PPF-19 patterns. The best synthetic condition for this phase (PPF-20) was obtained with a ratio of 1:3:3:4 (TCPP/Zn/DPNI/HNO_3) in DMF/ethanol (see Figure S3 in the Supporting Information for the X-ray powder pattern).

With the pillar DPT, the reactions of TCPP, $Zn(NO_3)_2 \cdot 6H_2O$, DPT, and HNO_3 in a molar ratio of 1:3:2:3 in DEF/ethanol (v/v 2:1) produced PPF-21 (see Figure S4 in the Supporting Information for the X-ray powder pattern). To prepare PPF-22, the same starting materials were dissolved in DMF/ethanol in a different molar ratio of 1:3:5:6 (TCPP/Zn/DPNI/HNO_3) (see Figure S5 in the Supporting Information for the X-ray powder pattern).

All PPF structures reported in this paper are based on a 2D porphyrin sheet (Figure 1), which is also a basic building unit in other 2D/3D PPFs previously reported.[12,13] The 2D porphyrin sheet contains Zn dinuclear paddlewheel SBUs that are bridged by four carboxylates from ZnTCPPs, forming planar sheetlike topology. Figure 2 shows a new 2D bilayer topology found in

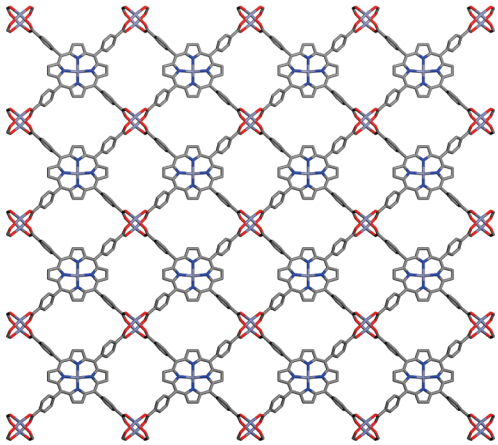

Figure 1. 2D porphyrin sheet commonly found in PPF series.

PPF-18 and PPF-21 with DPNI and DPT pillars, respectively. As can be seen in Figure 2, the pillars, DPNI (PPF-18) or DPT (PPF-21), are sandwiched by two porphyrin sheets resulting in a bilayer topology. Such bilayer structures are assembled by connecting the central Zn metal in TCPP and one of the axial sites of the Zn paddlewheel SBU by the pillar molecules. The other remaining axial position of the Zn paddlewheel site is occupied by water. Individual layers stack in an AB fashion. The variation in the lengths of the pillars is responsible for changes in crystallographic *c* parameters: 30.8966(6) Å for PPF-18 and 26.869(9) Å for PPF-21.

Interestingly, bilayer topology has not been observed in BPY-pillared paddlewheel PPFs.[12c,13] Instead, the BPY-pillared PPFs form an ABBA stacking pattern under similar synthetic conditions, as found in the PPF-4 case.[13] The bilayer topology is frequently found in nature. Examples include bilayer lipids,[22] which are fundamental building blocks in biological systems, and organic or metal−organic frameworks.[23−25] Ward and co-workers have reported numerous hydrogen-bonded bilayer phases based on guanidinium sulfonate moieties.[23] PPF-18 and PPF-21 structures are the first reported cases of bilayer formation among over 30 pillared paddlewheel frameworks reported to date.[7−10]

X-ray single crystal analysis reveals that PPF-19 has a distinct topology (Figure 3a), despite the fact that PPF-18 and PPF-19 both have the same stoichiometry. PPF-19 is a 3D pillared framework assembled from DPNI pillars connecting two axial positions of Zn paddlewheel SBUs in the porphyrin 2D sheets. The remaining Zn metal centers in the porphyrin core are capped by water molecules. The topology of PPF-19 can be best

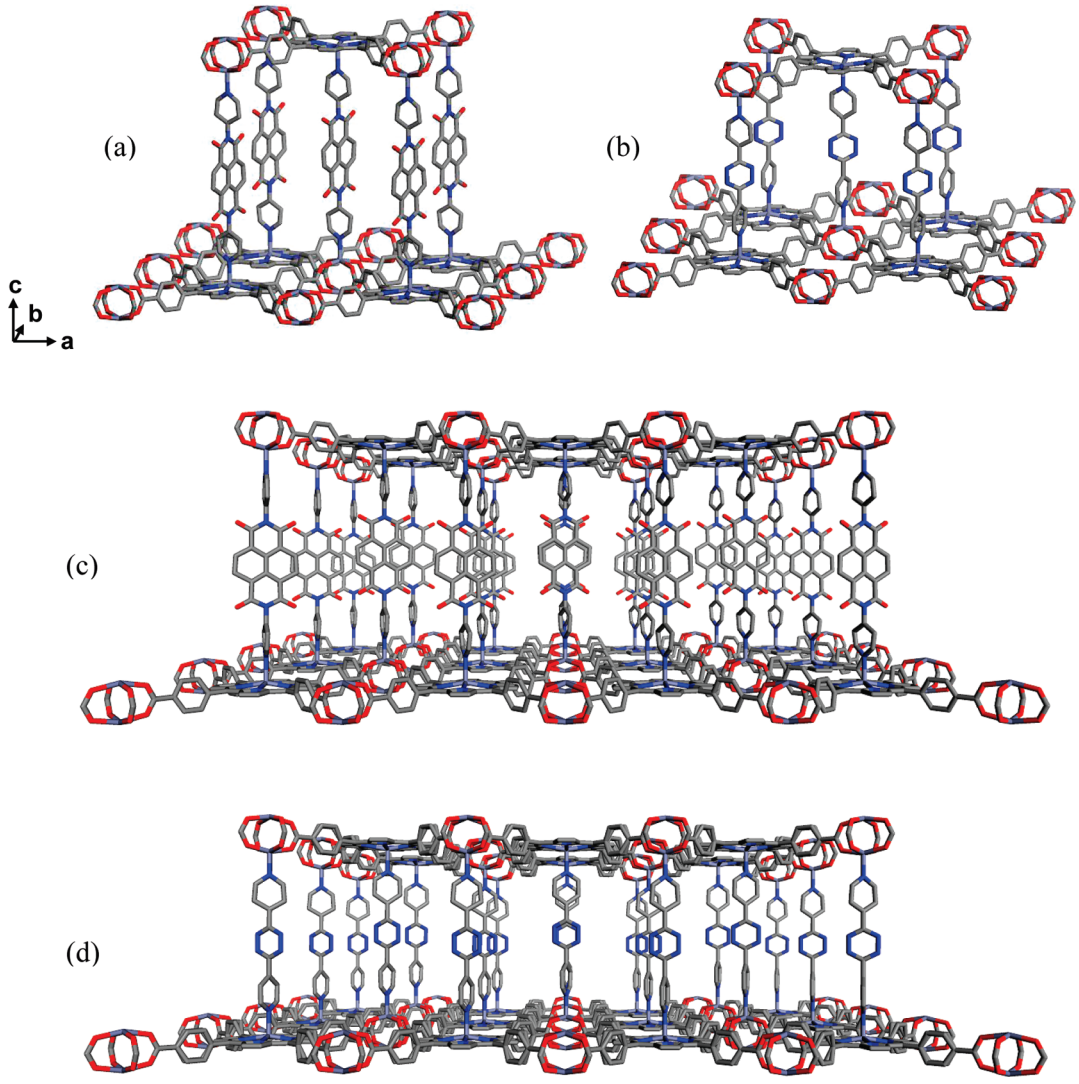

Figure 2. 2D bilayer structural motif found in (a) PPF-18 [Zn_2(ZnTCPP)(DPNI)] and (b) PPF-21 [Zn_2(ZnTCPP)(DPT)]. Perspective view of (c) PPF-18 and (d) PPF-21 along the [010] direction.

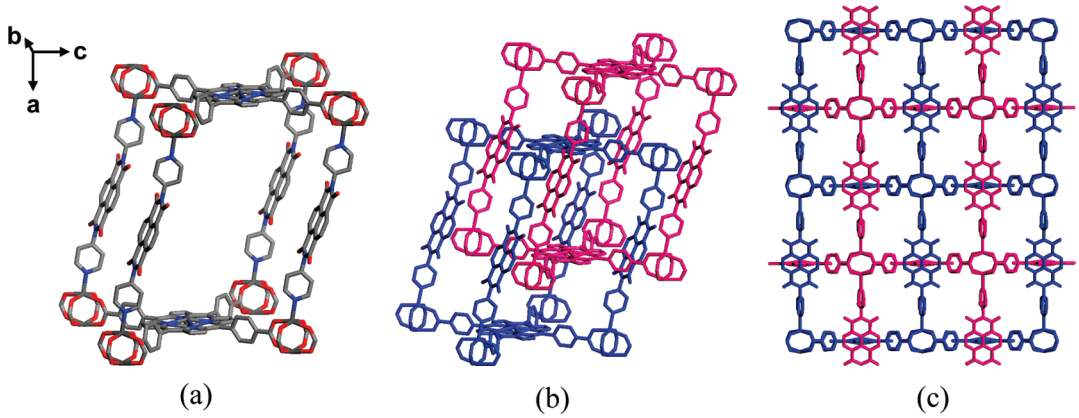

Figure 3. Single crystal structure of PPF-19 [Zn_2(ZnTCPP)(DPNI)]. (a) One of the two independent AA stacking nets, (b) two interpenetrating nets of PPF-19, and (c) [001] projection of 2-fold interpenetrating nets (colored in blue and pink).

Table 2. Examples of 3D Pillared Paddlewheel Frameworks[a]

	interpenetration	references
Zn_2(BDC)(TMBDC)(DABCO)	none	7a
Zn_2(TMBDC)$_2$(DABCO)	none	7a
Zn(1,4-NDC)$_2$(DABCO)	none	7a
Zn_2(TFBDC)$_2$(DABCO)	none	7a
Zn_2(TMBDC)$_2$(BPY)	none	7a
Zn_2(BDC)$_2$(DABCO)	none	7a−d
Cu_2(TFBDC)$_2$(DABCO)	none	7e
Zn_2(CAMPH)$_2$(DABCO)	none	7f
Zn_2(CAMPH)$_2$(BPY)	none	7f
Cu_2(MGLA)$_2$(BPY)	none	7g
Cu_2(GLA)$_2$(BPE)	none	7g
Zn_2(ADC)$_2$(DABCO)	none	7h
Cu_2(GLA)$_2$(BPY)	none	7i
Cu_2(GLA)$_2$(BPY-ETA)	none	7i
Ni_2(BODC)$_2$(DABCO)	none	7j
Ni_xCo_{2-x} (CAMPH)$_2$(DIMB)	none	7k
Zn_2(BDC)$_2$(BPY)	2-fold	7a,8a
Zn_2(FMA)$_2$(BPY)	2-fold	8a
Zn_2(BPDC)$_2$(DPNI)	2-fold	8a
Zn_2(2,6-NDC)$_2$(BPY)	2-fold	8a,b
Zn_2(2,6-NDC)$_2$(DPNI)	2-fold	8a,c
Co_2(2,6-NDC)$_2$(BPY)	2-fold	8d
Cu_2(FMA)$_2$(PYZ)	2-fold	8e
Cu_2(FMA)$_2$(BPE)	2-fold	8e
Cu_2(FMA)$_2$(BPY)	2-fold	8e,f
Zn_2(BPDC)$_2$(CDBS-Mn)	2-fold	8g
Zn_2(2,6-NDC)$_2$(BPE)	2-fold	8h
Cu_2(CDC)$_2$(BPY)	2-fold	8i
Cu_2(BPDC)$_2$(BPY)	2-fold	8j
Zn_2(2,6-NDC)$_2$(BPY)	3-fold	7a
Cd_2(BPDA)$_2$(BPY)	3-fold	9a
Zn_2(ABDC)$_2$(BPE)	3-fold	9b
Co_2(2,6-NDC)$_2$(BPE)	3-fold	9c
Co_2(2,6-NDC)$_2$(BPY)	3-fold	9d,e
Ni_2(2,6-NDC)$_2$(BPY)	3-fold	9d,e
Zn_2(CNC)$_2$(DPT)	3-fold	9f
Mn_2(ATP)$_2$(BPY-ETA)	3-fold	9g
Zn_2(BDC)$_2$(TAB)	3-fold	9h
Cd_2(BPDA)$_2$(BPE)	3-fold	9i

[a] ABDC = 4,4′-azobenzenedicarboxylate, ADC = 9,10-anthracenedicarboxylate, ATP = 2-aminoterephthalic, BDC = 1,4-benzenedicarboxylate, BPDA = 1,1′-biphenyl-3,3′-dicarboxylate, BPDC = 4,4′-biphenyldicarboxylate, BPE = *trans*-bis(4-pyridyl)ethylene, BPY = 4,4′-bipyridyl, BPY-ETA = 1,2-bis(4-pyridyl)ethane, BODC = 4,4′-bicyclo[2.2.2]octane, CAMPH = (+)-camphoric, CDBS-Mn = (*R*,*R*)-(−)-1,2-cyclohexanediamino-*N*,*N*′-bis(3-*tert*-butyl-5-(4-pyridyl)salicylidene)$Mn^{III}Cl$, CDC = *trans*-1,4-cyclohexanedicarboxylate, CNC = 4-carboxycinnamic, DABCO = 1,4-diazabicyclo[2.2.2]octane, DIMB = 1,4-di-(1-imidazolyl-methyl)benzene, DPNI = *N*,*N*′-di-(4-pyridyl)-1,4,5,8-naphthalenetetracarboxydiimide, DPT = 3,6-di-4-pyridyl-1,2,4,5-tetrazine, FMA = fumarate, GLA = glutarate, 1,4-NDC = 1,4-naphthalenedicarboxylate, 2,6-NDC = 2,6-naphthalenedicarboxylate, PYZ = pyrazine, MGLA = R-2-methylglutarate, TAB = 1,4-bis(1,2,4-triazol-1-yl)butane, TFBDC = tetrafluoroterephthalate, TMBDC = tetramethylterephthalate.

described as a (4,6) **fsc** net,[26] a rare net pattern assembled by 4-connected porphyrin linkers and 6-connected paddlewheel SBUs. A similar **fsc** net has been seen in BPY-pillared PPF-5 series, such as PPF-5-Pd/Co, PPF-5-Pt/Co, PPF-5-Ni/Zn, and PPF-V/Zn.[12c] Prior to this PPF series, this **fsc** net was rarely observed in the literature.[26] It is interesting to note that the difference between the PPF-5 series and new PPF-19 is the relative position of the pillars. In PPF-19, the DPNI pillars are slightly tilted. PPF-19 crystallizes in the monoclinic *C*2/*m*, unlike the PPF-5 series of *P*4/*mmm*.

Scheme 2. Organic Ligands and Pillars Used in 3D Pillared Paddlewheel Frameworks

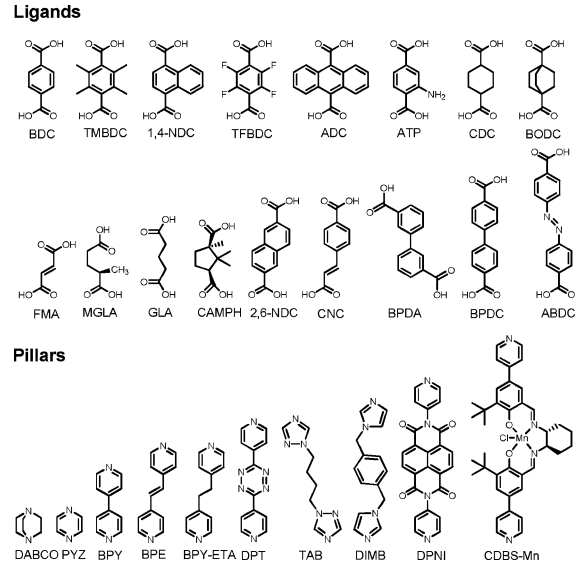

The structure of PPF-19 is further complicated by 2-fold interpenetration (Figure 3b,c).[27] Our previous work with the shorter BPY pillar has not yielded any interpenetrated PPF structures.[13] We also note a similar trend in the 3D pillared paddlewheel frameworks.[7−9] Table 2 shows 3D pillared paddlewheel frameworks, assembled from organic building blocks shown in Scheme 2. In general, when the pillar is small (e.g., DABCO), interpenetration is seldom observed.[28] However, as the pillar gets larger (e.g., BPY), a vast majority of pillared paddlewheel frameworks are doubly or even triply interpenetrated (Table 2). A notable difference between PPF-19 and the other interpenetrated paddlewheel-based MOFs is the interpenetration vector, which relates one net to the other interpenetrated net(s). Most paddlewheel-based, interpenetrated frameworks have interpenetration vectors aligned along the diagonal line of the rectangular net. Thus the vectors are (1/2, 1/2, 1/2) and (1/3, 1/3, 1/3) (Figure 4). However, the interpenetration vector

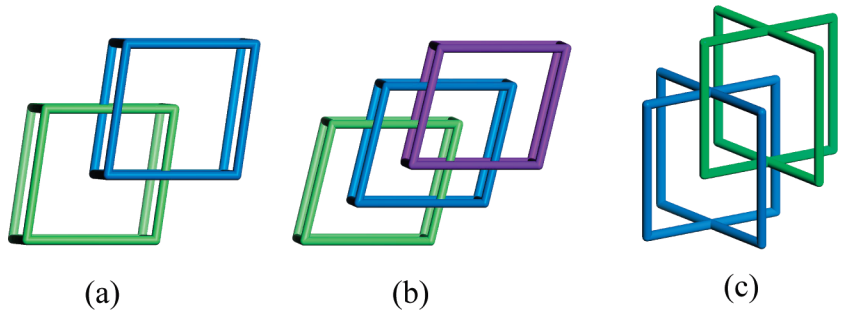

Figure 4. Interpenetrated nets found in pillared paddlewheel MOFs. (a) Two- and (b) 3-fold **pcu** nets,[8e,9a] and (c) 2-fold **fsc** net observed in PPF-19.

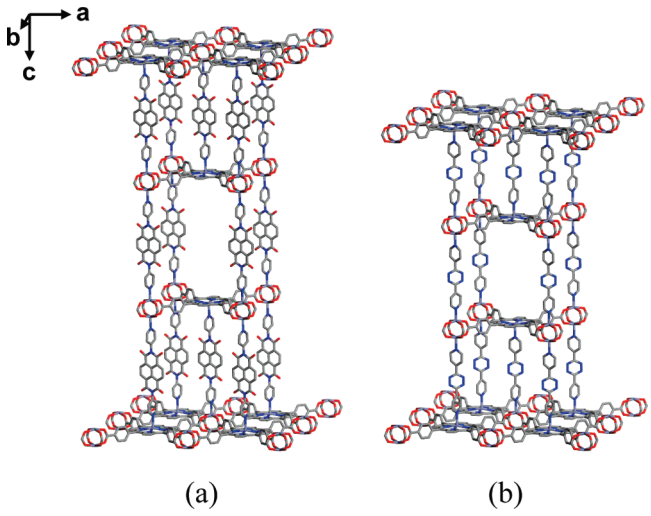

Figure 5. Single crystal structures of (a) PPF-20 [Zn_2(ZnTCPP)(DPNI)$_{1.5}$] and (b) PPF-22 [Zn_2(ZnTCPP)(DPT)$_{1.5}$].

Table 3. Summary of PPF Structures, Zn_2(ZnTCPP)(L)$_x$, L = BPY, DPT, DPNI

stacking pattern	x	DPNI (15.4 Å[a])	DPT (11.3 Å[a])	BPY (7.1 Å[a])[13]
AB bilayer	1.0	PPF-18	PPF-21	
AA interpenetration	1.0	PPF-19		
ABBA	1.5	PPF-20	PPF-22	PPF-4[13]

[a] The numbers in the parentheses indicate the length of the pillars used.

for PPF-19 is an exception; it is (1/2, 1/2, 0). The difference can be attributed to the shape of the porphyrin linker. Inherent D_{4h} symmetry of the porphyrin building block prevents the creation of another interpenetrated net along the diagonal line of the net. PPF-19 has the highest framework density (0.782 g/cm^3, calculated from single crystal data) among the PPFs structures that we have synthesized thus far.[12,13] Despite such interpenetration, PPF-19 still contains open channels. Although the positions of the framework atoms are readily solved from the X-ray single crystal refinement, the solvent molecules residing in the channels were not located, which is a common phenomenon in this type of MOF.

The framework topologies of PPF-20 and PPF-22 are based on an ABBA stacking pattern, isoreticular with the BPY-pillared PPF-4 previously reported (Figure 5).[13] The 2D porphyrin grids are pillared by DPNI (PPF-20) or DPT (PPF-22), connecting $Zn_2(COO)_4$ SBUs and porphyrin metal centers to form 3D frameworks with an ABBA stacking pattern. The crystallographic cell parameter c of PPF-20, 87.680(6) Å, is notably large due to the long DPNI pillar and the stacking sequence ABBA. The calculated framework density of PPF-20 is 0.437 g/cm^3, the lowest among the PPF structures thus far.[12,13] The crystallographic cell parameter c and the framework density of PPF-22 are 71.0521(18) Å and 0.449 g/cm^3, respectively. In this paper we observe three different structure types, AA, ABBA, and bilayer. The pillaring through synthetic conditions controls the stacking patterns of PPFs and therefore the final topologies. This variability is surprisingly different from other known 3D pillared paddlewheel frameworks as shown in Table 2. Previously reported frameworks are mostly topologically identical to a **pcu** net (or α-Po net).[7−9] The lack of topological variety in other 3D pillared paddlewheel frameworks is mainly because there exists only one pillaring site (i.e., the axial position of the paddlwheel SBUs) available in the frameworks. In contrast, the porphyrin 2D sheets provide an additional pillaring site in the porphyrin core. Having one more pillaring site creates interesting structural variation in PPF homologous series. The framework density can be tuned drastically as the structure changes. For example, in DPNI-based PPF series, the calculated framework density increases in the following order: 0.437 g/cm^3 (PPF-20), 0.546 g/cm^3 (PPF-18), 0.782 g/cm^3 (PPF-19) (Table 1).

We find an interesting trend in metal coordination and these three structure types (Table 3). Zn paddlewheel SBU and Zn metal in porphyrin core prefer six and five structural connectivity, respectively. The bilayer topology found in PPF-18 and PPF-21 has effectively five structural connections in the Zn paddlewheel.[29] To our surprise, the AA topology in PPF-19 has four connections in the porphyrin core,[30] as can be seen in the PdTCPP-based PPF-5.[23c] The ABBA stacking patterns in PPF-20 and PPF-22 contain 5-connecting Zn metal centers in the porphyrin and 6-connecting Zn paddlewheel motifs.

Conclusion

In summary, we have synthesized and structurally characterized a new PPF series using DPNI and DPT pillars via solvothermal reactions. We have identified two new PPF topologies, namely, bilayer and doubly interpenetrated AA stacking pattern, in addition to the ABBA pattern previously observed. Effective coordination numbers for the metal centers in the paddlewheel and the porphyrin vary from one structure to another, and therefore the resulting topologies are different. Extra binding centers for organic building blocks provide an exciting tunable feature in PPF topology.

Acknowledgment. The work is supported by Nebraska EPSCoR, Nebraska Center for Energy Sciences Research, Nebraska Center for Materials and Nanoscience, and University of Nebraska—Lincoln, Research Council. R.W.N. and H.-T.S. acknowledge the support from the UCARE program at University of Nebraska—Lincoln.

Supporting Information Available: Crystallographic data in CIF format and X-ray powder diffraction patterns. This material is available free of charge via the Internet at http://pubs.acs.org.

References

(1) (a) O'Keeffe, M.; Eddaoudi, M.; Li, H.; Reineke, T.; Yaghi, O. M. *J. Solid State Chem.* **2000**, *152*, 3. (b) Delgado-Friedrichs, O.; O'Keeffe, M.; Yaghi, O. M. *Acta Crystallogr.* **2006**, *A62*, 350. (c) Yaghi, O. M.; O'Keeffe, M.; Ockwig, N. W.; Chae, H. K.; Eddaoudi, M.; Kim, J. *Nature* **2003**, *423*, 705. (d) Férey, G. *Chem. Soc. Rev.* **2008**, *37*, 191.

(2) (a) Rowsell, J. L. C.; Yaghi, O. M. *Angew. Chem., Int. Ed.* **2005**, *44*, 4670. (b) Dincã, M.; Long, J. R. *Angew. Chem., Int. Ed.* **2008**, *47*, 6766. (c) Collins, D. J.; Zhou, H.-C. *J. Mater. Chem.* **2007**, *17*, 3154. (d) Férey, G.; Mellot-Draznieks, C.; Serre, C.; Millange, F.; Dutour, J.; Surblé, S.; Margiolaki, I. *Science* **2005**, *309*, 2040. (e) Rosi, N. L.; Eckert, J.; Eddaoudi, M.; Vodak, T.; Kim, J.; O'Keeffe, M.; Yaghi, O. M. *Science* **2003**, *300*, 1127. (f) Chen, B.; Zhao, X.; Putkham, A.; Hong, K.; Lobkovsky, E. B.; Hurtado, E. J.; Fletcher, A. J.; Thomas, K. M. *J. Am. Chem. Soc.* **2008**, *130*, 6411.

(3) (a) Seo, J. S.; Whang, D.; Lee, H.; Jun, S. I.; Oh, J.; Jeon, Y. J.; Kim, K. *Nature* **2000**, *404*, 982. (b) Kitagawa, S.; Kitaura, R.; Noro, S. *Angew. Chem., Int. Ed.* **2004**, *43*, 2334.

(4) (a) Maspoch, D.; Ruiz-Molina, D.; Wurst, K.; Domingo, N.; Cavallini, M.; Biscarini, F.; Tejada, J.; Rovira, C.; Veciana, J. *Nat. Mater.* **2003**, *2*, 190. (b) Janiak, C. *Dalton Trans.* **2003**, *14*, 2781.

(5) (a) Li, H.; Eddaoudi, M.; O'Keeffe, M.; Yaghi, O. M. *Nature* **1999**, *402*, 276. (b) Rowsell, J. L. C.; Eckert, J.; Yaghi, O. M. *J. Am. Chem. Soc.* **2005**, *127*, 14904.

(6) (a) Liu, Y.; Eubank, J. F.; Cairns, A. J.; Eckert, J.; Kravtsov, V. C.; Luebke, R.; Eddaoudi, M. *Angew. Chem., Int. Ed.* **2007**, *46*, 3278. (b) Surblé, S.; Serre, C.; Mellot-Draznieks, C.; Millange, F.; Férey, G. *Chem. Commun.* **2006**, 284. (c) Ma, S.; Wang, X.-S.; Manis, E. S.; Collier, C. D.; Zhou, H.-C. *Inorg. Chem.* **2004**, *46*, 3432. (d) Barthelet, K.; Riou, D.; Férey, G. *Chem. Commun.* **2002**, 1492.

(7) (a) Chun, H.; Dybtsev, D. N.; Kim, H.; Kim, K. *Chem.—Eur. J.* **2005**, *11*, 3521. (b) Dybtsev, D. N.; Chun, H.; Kim, K. *Angew. Chem., Int. Ed.* **2004**, *43*, 5033. (c) Uemura, K.; Yamasaki, Y.; Komagawa, Y.; Tanaka, K.; Kita, H. *Angew. Chem., Int. Ed.* **2007**, *46*, 6662. (d) Bárcia, P. S.; Zapata, F.; Silva, J. A. C.; Rodrigues, A. E.; Chen, B. *J. Phys. Chem. B* **2007**, *111*, 6101. (e) Kitaura, R.; Iwahori, F.; Matsuda, R.; Kitagawa, S.; Kubota, Y.; Takata, M.; Kobayashi, T. C. *Inorg. Chem.* **2004**, *43*, 6522. (f) Dybtsev, D. N.; Yutkin, M. P.; Peresypkina, E. V.; Virovets, A. V.; Serre, C.; Férey, G.; Fedin, V. P. *Inorg. Chem.* **2007**, *46*, 6843. (g) Chen, B.; Ji, Y.; Xue, M.; Fronczek, F. R.; Hurtado, E. J.; Mondal, J. U.; Liang, C.; Dai, S. *Inorg. Chem.* **2008**, *47*, 5543. (h) Tanaka, D.; Horike, S.; Kitagawa, S.; Ohba, M.; Hasegawa, M.; Ozawa, Y.; Toriumi, K. *Chem. Commun.* **2007**, 3142. (i) Rather, B.; Zaworotko, M. J. *Chem. Commun.* **2003**, 830. (j) Yuen, T.; Danilovic, D.; Li, K.; Li, J. *J. Appl. Phys.* **2008**, *103*, 07B725. (k) Zeng, M.-H.; Wang, B.; Wang, X.-Y.; Zhang, W.-X.; Chen, X.-M.; Gao, S. *Inorg. Chem.* **2006**, *45*, 7069.

(8) (a) Ma, B.-Q.; Mulfort, K. L.; Hupp, J. T. *Inorg. Chem.* **2005**, *44*, 4912. (b) Chen, B.; Liang, C.; Yang, J.; Contreras, D. S.; Clancy, Y. L.; Lobkovsky, E. B.; Yaghi, O. M.; Dai, S. *Angew. Chem., Int. Ed.* **2006**, *45*, 1390. (c) Mulfort, K. L.; Hupp, J. T. *J. Am. Chem. Soc.* **2007**, *129*, 9604. (d) Chen, B.; Ma, S.; Hurtado, E. J.; Lobkovsky, E. B.; Liang, C.; Zhu, H.; Dai, S. *Inorg. Chem.* **2007**, *46*, 8705. (e) Chen, B.; Ma, S.; Zapata, F.; Fronczek, F. R.; Lobkovsky, E. B.; Zhou, H.-C. *Inorg. Chem.* **2007**, *46*, 1233. (f) Dalai, S.; Mukherjee, P. S.; Zangrando, E.; Lloret, F.; Chaudhuri, N. R. *Dalton Trans.* **2002**, 822. (g) Cho, S.-H.; Ma, B.; Nguyen, S. T.; Hupp, J. T.; Albrecht-Schmitt, T. E. *Chem. Commun.* **2006**, 2563. (h) Chen, B.; Ma, S.; Zapata, F.; Lobkovsky, E. B.; Yang, J. *Inorg. Chem.* **2006**, *45*, 5718. (i) Chen, B.; Fronczek, F. R.; Courtney, B. H.; Zapata, F. *Cryst. Growth Des.* **2006**, *6*, 825. (j) Pichon, A.; Fierro, C. M.; Nieuwenhuyzen, M.; James, S. L. *CrystEngComm* **2007**, *9*, 449.

(9) (a) Wang, R.; Han, L.; Jiang, F.; Zhou, Y.; Yuan, D.; Hong, M. *Cryst. Growth Des.* **2005**, *5*, 129. (b) Chen, B.; Ma, S.; Hurtado, E. J.; Lobkovsky, E. B.; Zhou, H.-C. *Inorg. Chem.* **2007**, *46*, 8490. (c) Choi, E.-Y.; Park, K.; Yang, C.-H.; Kim, H.; Son, J.-H.; Lee, S. W.; Lee, Y. H.; Min, D.; Kwon, Y.-U. *Chem.—Eur. J.* **2004**, *10*, 5535. (d) Lee, S. W.; Kim, H. J.; Lee, Y. K.; Park, K.; Son, J.-H.; Kwon, Y.-U. *Inorg. Chim. Acta* **2003**, *353*, 151. (e) Hsu, L.-P.; Wu, J.-Y.; Lu, K.-L. *J. Inorg. Organomet. Polym. Mater.* **2007**, *17*, 259. (f) Xue, M.; Ma, S.; Jin, Z.; Schaffino, R. M.; Zhu, G.-S.; Lobkovsky, E. B.; Qiu, S.-L.; Chen, B. *Inorg. Chem.* **2008**, *47*, 6825. (g) Fu, Z.; Yi, J.; Chen, Y.; Liao, S.; Guo, N.; Dai, J.; Yang, G.; Lian, Y.; Wu, X. *Eur. J. Inorg. Chem.* **2008**, 628. (h) Wang, X.-L.; Qin, C.; Wang, E.-B.; Su, Z.-M. *Chem.—Eur. J.* **2006**, *12*, 2680. (i) Wang, R.; Hong, M.; Yuan, D.; Sun, Y.; Xu, L.; Luo, J.; Cao, R.; Chan, A. S. C. *Eur. J. Inorg. Chem.* **2004**, 37.

(10) Kitagawa, S.; Furukawa, S. In *Frontiers In Crystal Engineering*; Tiekink, E. R. T., Vittal, J. J., Eds.; Wiley: Hoboken, NJ, 2006; p 195.

(11) Kitagawa, S.; Noro, S.; Nakamura, T. *Chem. Commun.* **2006**, 701.

(12) (a) Choi, E.-Y.; Barron, P. M.; Novotny, R. W.; Hu, C.; Kwon, Y.-U.; Choe, W. *CrystEngComm* **2008**, *10*, 824. (b) Choi, E.-Y.; Wray, C. A.; Hu, C.; Choe, W. *CrystEngComm* **2009**, *11*, 553. (c) Barron, P. M.; Son, H.-T.; Hu, C.; Choe, W. *Cryst. Growth Des.* **2009**, *9*, 1960.

(13) Choi, E.-Y.; Barron, P. M.; Novotny, R. W.; Son, H.-T.; Hu, C.; Choe, W. *Inorg. Chem.* **2009**, *48*, 426.

(14) (a) Sanders, J. K. M.; Bampos, N.; Cyde-Watson, Z.; Darling, S. L.; Hawley, J. C.; Kim, H.-J.; Mak, C. C.; Webb, S. J. In *Porphyrin Handbook*; Kadish, K.; Smith, K., Guilard, R., Eds.; Academic Press: New York, 2000; Vol. 3, p 1. (b) Chou, J.-H.; Kosal, M. E.; Nalwa, H. S.; Rakow, N. A.; Suslick, K. S. In *Porphyrin Handbook* Kadish, K., Smith, K., Guilard, R., Eds.; Academic Press: New York, 2000; Vol. 6, p 43. (c) Suslick, K. S.; Bhyrappa, P.; Chou, J. H.; Kosal, M. E.; Nakagaki, S.; Smithenry, D. W.; Wilson, S. R. *Acc. Chem. Res.* **2005**, *38*, 283. (d) Drain, C. M.; Goldberg, I.; Sylvain, I.; Falber, A. *Top. Curr. Chem.* **2005**, *245*, 55 (e) Goldberg, I. *Chem. Commun.* **2005**, *1243*. (f) Kosal, M. E.; Chou, J. H.; Wilson, S. R.; Suslick, K. S. *Nat. Mater.* **2002**, *1*, 118. (g) DeVries, L. D.; Choe, W. *J. Chem. Crystallogr.* **2009**, *39*, 229.

(15) *SMART (version 6.532). Program for Bruker CCD X-ray Diffractometer Control, Bruker AXS Inc.*, Madison, WI, 2005.

(16) *SAINT+ (version 6.45). Program for Reduction of Data Collected on Bruker CCD Area Detector Diffractometer*; Bruker AXS Inc.: Madison, WI, 2003.

(17) Sheldrick, G. M. *SADABS, version 2.10, Program for Empirical Absorption Correction of Area Detector Data*; University of Göttingen: Göttingen, 2007.

(18) Sheldrick, G. M. *SHELXTL, version 6.14, Program Package for Structure Solution and Refinement*; *Bruker Analytical X-ray Systems, Inc.*: Madison, WI, 2003.

(19) Spek, A. L. *J. Appl. Crystallogr.* **2003**, *36*, 7.

(20) DPNI was synthesized acoording to the established method. See Gorteau, V.; Bollot, G.; Mareda, J.; Perez-Velasco, A.; Matile, S. *J. Am. Chem. Soc.* **2006**, *128*, 14788.

(21) Due to the purity of the product, yield is not calculated. See Results and Discussion section for details.

(22) (a) Ringsdorf, H.; Schlarb, B.; Venzmer, J. *Angew. Chem., Int. Ed.* **1988**, *27*, 113. (b) Kunitake, T. *Angew. Chem., Int. Ed.* **1992**, *31*, 709. (c) Fuhrhop, J.-H.; Helfrich, W. *Chem. Rev.* **1993**, *93*, 1565.

(23) (a) Horner, M. J.; Holman, K. T.; Ward, M. D. *J. Am. Chem. Soc.* **2007**, *129*, 14640. (b) Martin, S. M.; Yonezawa, J.; Horner, M. J.; Macosko, C. W.; Ward, M. D. *Chem. Mater.* **2004**, *16*, 3045. (c) Martin, S. M.; Ward, M. D. *Langmuir* **2005**, *21*, 5324.

(24) (a) Zaworotko, M. J. *Chem. Commun.* **2001**, *1*. (b) Power, K. N.; Hennigar, T. L.; Zaworotko, M. J. *New J. Chem.* **1998**, 177. (c) Kepert, C. J.; Rosseinsky, M. J. *Chem. Commun.* **1999**, 375. (d) Kondo, M.; Yoshitomi, T.; Seki, K.; Matsuzaka, H.; Kitagawa, S. *Angew. Chem., Int. Ed.* **1997**, *36*, 1725.

(25) (a) Maji, T. K.; Ohba, M.; Kitagawa, S. *Inorg. Chem.* **2005**, *44*, 9225. (b) Lin, J.-G.; Xu, Y.-Y.; Qiu, L.; Zang, S.-Q.; Lu, C.-S.; Duan, C.-Y.; Li, Y.-Z.; Gao, S.; Meng, Q.-J. *Chem. Commun.* **2008**, 2659.

(26) This **fsc** net is theoretically reported by O'Keeffe and experimentally observed for the first time by Bi et al. See: (a) Bi, M.; Li, G.; Hua, J.; Liu, Y.; Liu, X.; Hu, Y.; Shi, Z.; Feng, S. *Cryst. Growth Des.* **2007**, *7*, 2066. (b) Shultz, A. M.; Farha, O. K.; Hupp, J. T.; Nguyen, S. T. *J. Am. Chem. Soc.* **2009**, *131*, 4204.

(27) For reviews on interpenetration, see: (a) Batten, S. R. *CrystEngComm* **2001**, *3*, 67. (b) Batten, S. R.; Robson, R. *Angew. Chem., Int. Ed.* **1998**, *37*, 1460. (c) Batten, S. R. Monash University, Australia, 2008, http://www.chem.monash.edu.au/staff/sbatten/interpen/index.html.

(28) Although PYZ pillar is similar in size with DABCO, a 2-fold interpenetration is found in $Cu_2(FMA)_2(PYZ)$.[8e]

(29) One of the axial positions in the Zn paddlewheel is capped by a water molecule. For an example of 5-connecting Cu paddlewheel motif, see: (a) Chun, H.; Jung, H.; Seo, J. *Inorg. Chem.* **2009**, *48*, 2043.

(30) Zn metal in the porphyrin core is coordinated by a water molecule.

CG900220G